For submission to Water Research as a Full Paper

Photosynthesis in sediments determined at high spatial resolution by the use of microelectrodes

Short running title: Photosynthesis in sediments

By

YOSHIYUKI NAKAMURA [1], **HISASHI SATOH** [2*], **SATOSHI OKABE** [1] and **YOSHIMASA WATANABE** [1]

[1]*Department of Urban and Environmental Engineering, Graduate school of Engineering, Hokkaido University, Sapporo 060-8628, Japan.*

[2]*Department of Environmental and Civil Engineering, Hachinohe Institute of Technology, Hachinohe, Aomori 031-8501, Japan.*

- *Corresponding Author*
  - *Hisashi SATOH*
  - *Department of Environmental and Civil Engineering, Hachinohe Institute of Technology, 88-1 Ohbiraki, Myo, Hachinohe, Aomori 031-8501, Japan.*
  - *Tel.: +81-(0)178-25-8067*
  - *Fax.: +81-(0)178-25-0722*
  - *E-mail: qsatoh@hi-tech.ac.jp*

Abstract

The present study investigated photosynthetic rates and their regulation by light within the upper 5 mm of sediment in a tidal area of Niida River in Hachinohe, Japan. Steady-state concentration profiles of O_2, NH_4^+, NO_2^-, H_2S, and pH in the sediment were measured with microelectrodes. Microzonation of O_2 respiration, denitrification and SO_4^{2-} reduction was found in the sediment. When light intensities exceeded 1050 μmol photons/m^2/s, net photosynthetic activity was detected in the upper 0.5 mm of the microbial mat colonizing on the sediment surface in the tidal area. In contrast, gross photosynthetic activity was detected in the upper 1.0 mm of the microbial mat at 1900 μmol photons/m^2/s. As light intensity increased, the net photosynthetic rate and O_2 penetration depth increased. The maximal net photosynthetic rate and O_2 penetration depth were 6.1 μmol O_2/cm^3/h and 2.2 mm, respectively, at 1900 μmol photons/m^2/s. Net photosynthetic rates in the microbial mat in the tidal area were lower than in the upstream sediment. The analysis of continuous O_2 concentration measurements in different layers of the microbial mat during artificial light-dark cycles demonstrated that the photosynthetic activity response to changes in light intensity was extremely fast (a few seconds) and the O_2 concentration in the microbial mat became stable within 200 s. The measurement of physical and chemical parameters in river water revealed that the study site was relatively polluted and sunlight intensity significantly fluctuated temporally. These results suggested that the in situ microbial processes occurring in the sediment fluctuated in accordance with periodic fluctuations in sunlight intensity.

Key words

Photosynthesis; Light intensity; River sediment; Tidal area; Microelectrodes

Introduction

Photosynthesis significantly affects carbon and nitrogen cycles in river systems (Falkowski and Raven, 1997b). While the primary photosynthetic microorganisms in the sea are planktonic microalgae, in rivers photosynthetic microorganisms in microbial mats,

which colonize on sediment surface, and in epilithic biofilms that grow on stones, are significant contributors to photosynthetic activity. The microbial mats are compact microbial communities with high specific rates of metabolic processes (Castenholz, 1994). The high rates are due to dense populations of microorganisms and the high availability of organic carbon and nutrients. Photosynthetic microorganisms in the microbial mats act as sources of organic carbon and oxygen (O_2). In addition, the microbial mats receive organic carbon and nutrients from overlying water.

Although the typical thickness of a microbial mat is only a few millimeters, a vertical zonation of the microbial processes can be found in the microbial mat (Jensen *et al.*, 1994; Wieland and Kühl, 2000). The use of microelectrodes has made it possible to study such microzonation of the microbial processes and the tight spatial coupling between them at high spatial resolution. The O_2 respiration process affected nitrification and denitrification in freshwater sediment (Jensen *et al.*, 1994), sulfate (SO_4^{2-}) reduction in a hot spring cyanobacterial mat (Wieland and Kühl, 2000), and photosynthesis in hypersaline microbial mats (Grötzschel and de Beer, 2002).

In the river systems, oxygenic photosynthesis, followed by increases in O_2 and organic carbon concentrations, affects the microbial processes in the sediment. Although the thickness of the photosynthetic zone is less than one millimeter due to limited light penetration in the sediment, the specific photosynthetic rate is very high. Microelectrode measurements have revealed the occurrence of oxygenic photosynthesis with high photosynthetic rates in cyanobacterial mats (Wieland and Kühl, 2000; Ramsing *et al.*, 2000) and natural biofilms (Glud *et al.*, 1992). Light (Ramsing *et al.*, 2000), O_2 concentration (Grötzschel and de Beer, 2002) and temperature (Wieland and Kühl, 2000) affect the photosynthetic activity in the cyanobacterial mats. However, very little is known about the microbial processes and the effect of environmental factors in sediment at a river mouth.

Rivers flowing through urban areas receive anthropogenic inputs of organic carbon and nutrients (e.g. nitrogen and phosphorus) from adjacent land (Chen *et al.*, 1999; Sørensen and Revsbech, 1990). At the river mouth, diverse physical and chemical factors (e.g. sunlight, concentrations of organic carbon and nutrients, changes in flow rates and salinity), as well as nutrient retention occur because of tides (Feng *et al.*, 2002). These environmental factors could affect the microbial photosynthesis, O_2 respiration,

nitrification, denitrification, and SO_4^{2-} reduction. Therefore, the microbial processes in the sediment of a tidal area may be spatially and temporally dynamic when compared with other environments.

In the present study, we investigated the effect of light intensity on the net photosynthetic activity of sediment located in a tidal area of the Niida River, Hachinohe, Japan. We further discussed the effect of light intensity on microzonation of the microbial processes. Laboratory measurements of the O_2, NH_4^+, NO_2^-, H_2S, and pH concentration profiles, and net and gross photosynthetic rates were performed with microelectrodes. Furthermore, river water quality and environmental conditions of the sediments were determined.

2. Materials and methods

2.1. Sampling

Sediment samples and river water were collected at two points (Point 1 and 2) in the Niida River in Hachinohe, Japan (Fig. 1). The Niida River flows through agricultural areas and a city area in Hachinohe. The population of Hachinohe City is about 245,000. There are several factories of processed marine products around the downstream part of the Niida River. River water samples were collected during April and December 2002. Flow rate at the point 2 ranged from 212 to 2.3 m^3/s during the study period and the average was 15 m^3/s. Maximal tidal range is 130 cm. The point 1 and 2 are located approximately 1.5 and 8.0 km from the river mouth, respectively. Sediment samples were collected using 4 cm diameter Plexiglas tubes with minimal disturbance. The sediment and river water samples were transferred to the laboratory and were analyzed within 12 h using the methods described below.

2.2. Microelectrode measurements

In the laboratory, steady state concentration profiles of O_2, NH_4^+, NO_2^-, H_2S, and pH in the sediments were recorded according to the protocol reported elsewhere (Satoh *et al.*,

2003). Clark-type microelectrodes for O_2 with a tip diameter of approximately 15 μm and a 90 % response time <0.5 s were prepared and calibrated as described by Revsbech (Revsbech, 1989). LIX-type microelectrodes for NH_4^+, NO_2^- and pH (de Beer *et al.*, 1997) were constructed, calibrated, and used according to a protocol reported elsewhere (Okabe *et al.*, 1999b). H_2S microelectrodes were constructed as described by Revsbech *et al.* (1983) and were calibrated and used as described elsewhere (Okabe *et al.*, 1999a).

A flow cell reactor (60 (L) × 10 (W) × 5 (H) cm) for microelectrode measurements was constructed using an acrylic board (Fig. 2). The sediment samples were positioned in the reactor, where the surface of the microbial mat colonizing on the sediment surface was aligned with the bottom of the flow cell. 5.0 liter of the medium for microelectrode measurements was fed to the reactor at an average liquid velocity of 2 cm/s. To create a parallel, nonturbulent flow, a metallic net was mounted at the upstream of the reactor. The depth of the water above the microbial mat surface was about 1 cm. For the measurements of O_2 concentration profiles in the sediment, raw river water sampled at the sampling points was used as the medium for microelectrode measurements. Light intensity was changed from 10 to 1900 μmol photons/m^2/s. When the microprofiles of NH_4^+, NO_2^-, H_2S, and pH in the sediment were measured, a synthetic medium was used to avoid interference with the LIX-type microelectrodes. The synthetic medium consisted of NH_4Cl (50 μM), $NaNO_2$ (40 μM), $NaNO_3$ (100 μM), Na_2SO_4 (2000 μM), Na_2HPO_4 (3000 μM), $MgCl_2 \cdot 6H_2O$ (84 μM), $CaCl_2$ (200 μM), EDTA (270 μM). pH was adjusted to 7.5. Light intensity was adjusted to 10 μmol photons/m^2/s. The sediment was then acclimated in the medium at 20°C for at least 30 minutes before measurements to ensure that steady-state profiles were obtained. The microelectrodes were mounted on a motor-driven micromanipulator for accurate positioning and the concentration profiles in the sediment were recorded at intervals of 0.05 to 0.3 mm from the bulk liquid into the sediment (Okabe *et al.*, 1999b). The microbial mat surface was determined by using a dissection microscope (model Stemi 2000; Carl Zeiss). Halogen lamps supplied needed light during the experiments. At least three concentration profiles were measured at different positions in the sediment for each species and set of conditions. When O_2 concentrations were measured during artificial light-dark cycles, the sediment was illuminated at 1900 μmol photons/m^2/s for 10 minutes and the electrode was introduced into the sediment. The sediment was then shaded and kept in the dark until the O_2

concentration became stable. The sediment was then illuminated again at 1900 µmol photons/m^2/s and kept in the light until the O_2 concentration became stable. After two light-dark cycles, the electrode was introduced into deeper layers.

2.3. Calculation of metabolic rates

Net specific rates of O_2 production (P_{net}) or O_2 consumption (C_{net}) in the sediments were calculated from the mean steady state concentration profiles using Fick's second law of diffusion including a production or a consumption term:

$$Ds\ (d^2Cs(z)/dz^2) = C_{net} \text{ or } - P_{net}$$

where Ds is the effective sediment diffusion coefficient for O_2 and Cs(z) is the O_2 concentration at depth z. The details of this method were described previously by Lorenzen *et al.* (1998).

The Ds was calculated from the free solution molecular diffusion coefficient (D_0) for O_2 and the sediment porosity (ϕ) according to Ullman and Aller (1982):

$$Ds = \phi^2 D_0$$

The D_0 for O_2 (2.09×10^{-5} cm^2/s) at 20°C was found in the literature (Andrussow, 1969). Porosity and Ds at relevant depths of the investigated sediments are summarized in Table 2.

Gross photosynthetic rates (P_{gross}) were determined with same O_2 microelectrodes by the light-dark-shift method (Revsbech and Jørgensen, 1983; Revsbech *et al.*, 1981), in which the decrease in O_2 concentration was determined during a 2 s dark period and the P_{gross} at each depth could be calculated from the following equation:

$$P_{gross} = - dCs(t)/dt$$

where dCs(t)/dt is the rate of O_2 disappearance during 2 s after darkening. Theory of this method was described elsewhere (Revsbech *et al.*, 1981). A short summary is given here. A steady state O_2 profile in the sediment will be approached after a long period of illumination. At steady state, the photosynthetic O_2 production in any layer will balance the combined losses due to respiration and to diffusion of O_2 away from that layer (calculated negative if there is a net diffusion to the layer). When illumination is suddenly stopped, diffusion and respiration are initially unchanged, so that the O_2 concentration in the layer will decrease at a rate equal to the former photosynthetic rate. Furthermore, specific O_2 respiration rates

(R_{O2}) were calculated from these rates by subtracting the P_{net} from the P_{gross} for each layer of the sediment.

2.4. Analytical methods

Chemical Oxygen Demand (COD), using $KMnO_4$ as an oxidant, Biochemical Oxygen Demand (BOD) and Dissolved Organic Carbon (DOC) were analyzed according to the Standard Methods (APHA, 1998). The NH_4^+ and NO_2^- concentrations were determined colorimetrically. The NO_3^- and SO_4^{2-} concentration was determined using an ion chromatograph (HIC-6A; Shimadzu) equipped with a Shim-pack IC-A1 column. The samples for NH_4^+, NO_2^-, NO_3^- and SO_4^{2-} were filtered with 0.2 μm membrane filters before analysis. Porosity of the sediment was analyzed according to the methods of Murdroch and Azcue (1995). Ignition loss was measured from the loss of volatile matter upon ignition at 600˚C for 2 h. Total iron (T-Fe) concentration in the sediment was analyzed using an atomic adsorption spectrophotometer (AA-670; Shimadzu) after a proper sample pretreatment (APHA, 1998). Light intensity was measured by a quantum meter (Fujiwara Scientific Company), which senses only in the 400 to 700 nm region. All measurements were made above the water surface. Salinity was measured using a salinometer. The O_2 concentration and pH were determined using an O_2 electrode and a pH electrode, respectively.

3. Results and discussion

3.1. Physical and chemical parameters in river water and sediments at the study sites

Physical and chemical parameters (average ± standard deviation) of the river water (n=57) at the point 1 are shown in Table 1. The river water quality at the point 1 was relatively polluted while BOD was low and the NH_4^+ concentration was below the detection limit at the point 2 (data not shown). The average NO_3^- concentration was 127 μM at the point 1. SO_4^{2-} concentrations and salinity fluctuated, indicating that the point 1 was located in a tidal area. The sediment located at the point 1 was exposed to atmosphere for several hours during the spring tide. The sediment at the point 1 consisted of sand and the sediment

at the point 2 consisted of silt (Murdroch and Azcue, 1995). A ca. 1 mm thick brownish microbial mat colonized on the sediment surface at the point 1. A black layer underlay the microbial mat, indicating the precipitation of iron sulfide (FeS) in the sediment. Average values of porosity and Ds for O_2, which was calculated from the molecular diffusion coefficient for O_2 in water and the average value of porosity, at relevant depths of the investigated sediments are summarized in Table 2. The average value of porosity (n=6) slightly decreased with depth. Ignition loss in the upper 5 mm of the sediments at the point 1 and point 2 (n=6) was 4.8 ± 0.5 % and 3.4 ± 0.5 %, respectively. Benthic animals (*Tylorrhynchus heterochaetus*) were found at a density of about 2,000 individuals/m^2 in the sediment at the point 1. The average concentration profile of T-Fe in the sediment at the point 1 (n=6) is shown in Fig. 3. The average T-Fe concentration was 21 mg/g dry weight in the microbial mat. The T-Fe concentration slightly increased with depth and the maximum concentration was 25 ± 12 mg/g at a depth of 4-5 mm.

The diurnal cycle of sunlight intensity on the surface of the sediment at the point 1 in June 2003 is shown in Fig. 4. The light intensity increased as the sun rose and reached its maximum (1920 μmol photons/m^2/s) just before noon on sunny days. The light intensity then gradually decreased during the afternoon. The light intensities on cloudy days showed the same trend, but were less than half of the light intensities on sunny days. Even on sunny days, when clouds shaded the sediment surface, the light intensity decreased to the level of cloudy days within a few seconds.

3.2. Concentration profiles in sediments

Representative 2-D contour plots of O_2 in the sediment at the point 1 at 10 μmol photons/m^2/s, constructed from 11 vertical O_2 profiles, are shown in Fig. 5. The sediment sample was collected on 6 June 2001. The O_2 concentration in the bulk liquid was ca. 130 μM. O_2 decreased in the diffusive boundary layer above the microbial mat. The O_2 concentrations at the microbial mat surface were almost the same (90 μM) at all measuring points. The contour lines of 10, 30 and 60 μM of O_2 followed the microbial mat surface.

Mean steady-state concentration profiles of O_2, NH_4^+, NO_2^-, H_2S, and pH in the sediment at the point 1 at 10 μmol photons/m^2/s are shown in Fig. 6. The sediment sample

was collected on 23 January 2002. O_2 penetrated 1.3 mm into the microbial mat. The NH_4^+ produced in deeper parts of the sediment diffused toward the microbial mat and was consumed in the microbial mat. NO_2^- concentration decreased in the upper parts of the oxic zone due to nitrification. NO_2^- concentration profile showed a peak of ca.150 μM at a depth of 1.0 mm. Decreased NO_2^- concentrations in the lower parts of the oxic zone and anoxic sediment were probably due to denitrification. H_2S was detected in the sediment below a depth of 3.0 mm, indicating SO_4^{2-} reduction occurred in this zone. These results clearly indicate the microzonation of O_2 respiration, denitrification and SO_4^{2-} reduction in the upper 5 mm of the microbial mat and sediment. Decrease in H_2S concentration at a depth of 2.7 mm could be explained by H_2S oxidation by NO_2^- and NO_3^- and H_2S fixation with Fe. The abundance of T-Fe in the deeper parts of the sediment (Fig. 3) reflected this result.

3.3. Effect of light intensity on O_2 concentration profiles and photosynthesis in the sediments

The effects of oxygenic photosynthesis on O_2 concentration in the sediments at the point 1 were investigated because O_2 concentration affected the microzonation of O_2 respiration, denitrification and SO_4^{2-} reduction (Jensen *et al.*, 1994; Wieland and Kühl, 2000). Mean steady-state O_2 concentration profiles measured at five different light intensities and calculated net rates of O_2 production (P_{net}) and O_2 consumption (C_{net}) in the sediment are shown in Fig. 7A to 7E. The sediment sample was collected on 1 July 2003. The photosynthetic activities were detected in the upper 0.5 mm of the microbial mat when light intensities were more than 1050 μmol photons/m^2/s. As light intensity increased, the P_{net} in the microbial mat increased, resulting in increases in O_2 penetration depth and maximal O_2 concentration in the sediment. The maximal O_2 concentration in the microbial mat increased to 240 μM at a depth of 0.2 mm at 1900 μmol photons/m^2/s, which was 1.4 times higher than that of the bulk liquid. In this layer the P_{net} was 6.1 μmol O_2/cm^3/h. The average O_2 penetration depth at 1900 μmol photons/m^2/s was 2.2 mm, which was about three times deeper than in the sediment at 10 μmol photons/m^2/s (Fig. 7A). These results indicate that in nature, the O_2 penetration depth in the sediment could change from ca. 0.7 mm to ca. 2.2 mm in accordance with fluctuations in sunlight intensity (Fig. 4).

Increase in O_2 penetration depth results in higher redox potential in the upper parts of the sediment (Jørgensen *et al.*, 1979) and a shift in the zones of anoxic microbial processes (i.e. denitrification and SO_4^{2-} reduction) to the deeper layers of the sediment (Jensen *et al.*, 1994; Wieland and Kühl, 2000). In this study, microzonation of O_2 respiration, denitrification and SO_4^{2-} reduction was found in the sediment (Fig. 6). Consequently, the locations of the zones of anoxic microbial processes should fluctuate in accordance with a diurnal cycle of sunlight intensity. In the deeper parts of the sediment, the metabolic rates were low because biodegradable organic carbon and nutrients were usually limited due to the long diffusional distance from overlying water, although limited nutrients were supplied from below. Therefore, denitrification and SO_4^{2-} reduction rates might be higher during the night as compared with in the daytime. These results indicate that fluctuations in sunlight intensity might indirectly affect the carbon and nitrogen cycles in the sediment. However, many physical and chemical factors (e.g. vertical hydraulic flow within pores of the sediment induced by tide, water turbulence on the sediment surface, and fluctuations in organic carbon and nutrient concentrations in river water) affect O_2 distribution in the sediment in nature. Consequently, our results present the mechanism of change in O_2 distribution in the sediment by light rather than O_2 concentration profiles in the sediment in nature.

C_{net} was high just below the net O_2 production zone. With increasing light intensity, the maximal C_{net} increased; the C_{net}s were 0.7, 1.3 and 1.8 μmol $O_2/cm^3/h$ at 1050, 1550 and 1900 μmol photons/m^2/s, respectively. This was probably due to increasing concentrations of O_2 and organic carbon provided from photosynthetic zone in this zone.

The profiles of the average gross photosynthetic rate (P_{gross}) and O_2 respiration rate (R_{O2}) in the sediment at the point 1 at 1900 μmol photons/m^2/s are shown in Fig. 8. The sediment sample was collected on 16 July 2003. The R_{O2} was calculated by subtracting the P_{net} shown in Fig. 7E from the P_{gross}. The P_{gross} peaked at a depth of 0.2 mm with the rate of 8.6 μmol $O_2/cm^3/h$ and then decreased gradually with depth. Gross photosynthesis occurred from the surface to a depth of 1.0 mm, while the net photosynthesis was detected in the upper 0.5 mm of the microbial mat (Fig. 7E). This indicates that the photic zone ranged from the surface to a depth of 1.0 mm. The R_{O2}s in the photic zone were below 2.9 μmol $O_2/cm^3/h$. These values were comparable with the C_{net}s in the sediment at 10 μmol photons/m^2/s (Fig.

7A).

Representative steady-state O_2 concentration profiles measured at five different light intensities and P_{net} and C_{net} in the sediment located at the point 2 are shown in Fig. 9A to 9E. The sediment sample was collected on 9 September 2001. The P_{net} in the sediment at the point 2 was higher than in the sediment at the point 1 (Fig. 7). In the sediment photosynthesis occurred even at 100 μmol photons/m^2/s (Fig. 9B). The P_{net} (6.6 μmol O_2/cm^3/h) at 100 μmol photons/m^2/s was highest at a depth of 0.1 mm in the sediment. This value was higher than in the sediment at the point 1 at 1900 μmol photons/m^2/s (Fig. 7E). With increasing light intensity, the maximal P_{net} in the sediment at the point 2 increased. The P_{net} increased to 13.2 μmol O_2/cm^3/h at a depth of 0.1 mm at 1250 μmol photons/m^2/s. The difference in the photosynthetic rates between these two types of sediment may be attributed to difference in photosynthetic microorganisms between the sampling sites, although the photosynthetic microorganisms in the sediments were not investigated.

Continuous readings of O_2 concentrations in different layers of the sediment at the point 1 during artificial light-dark cycles are shown in Fig. 10A to 10D. The sediment sample was collected on 1 August 2003. At depths of 0.2, 0.4 and 0.6 mm, the O_2 concentration immediately decreased after darkening (0 s) and became stable within 200 s. Thereafter, when the sediment was illuminated again, the O_2 concentration increased immediately at depths of 0.2 and 0.4 mm, however, a small lag (a few seconds) occurred before O_2 started to increase at a depth of 0.6 mm (Fig. 10D). The steady-state O_2 concentration in the light gradually decreased as the light-dark cycle progressed. This was significant in the deeper layers, that is, in the later measurements. The possible explanations for a decrease in the maximal O_2 concentration might be an inherent circadian rhythm of the photosynthetic microorganisms (Falkowski and Raven, 1997a), migration of photosynthetic microorganisms into deeper layers of the sediment (Ramsing *et al.*, 2000), and/or increased photorespiration (Glud *et al.*, 1992).

Conclusions

Photosynthetic activities in the sediment in the tidal area of Niida River in Hachinohe, Japan, were determined at high spatial resolution by microelectrode technique.

Photosynthesis occurred in the upper 0.5 mm of the sediment. Microelectrode measurements revealed that a vertical microzonation of O_2 respiration, denitrification and SO_4^{2-} reduction was found in the upper 5 mm of the sediment. As light intensity increased, the net photosynthetic rate and O_2 penetration depth in the sediment increased. Consequently, the location and activities of anoxic microbial processes occurring in the sediment could fluctuate in accordance with periodic fluctuations in sunlight intensity.

References

Andrussow L. (1969) Diffusion. In *Landolt-Bornstein Zahlenwerte und Functionen. vol. II/5a*, eds. Borchers H., Hauser H., Hellwege K. H., Schafer K. and Schmidt E. Springer, Berlin, Germany.

APHA, AWWA and WEF. (1998) *Standard Methods for the examination of water and wastewater* (20th edn.). American Public Health Association, Washington, DC.

Castenholz R. W. (1994) Microbial mat research: The recent past and new perspectives. p. 3-18. In *Microbial mats: structure, development and environmental significance,* eds. Stal L. J. and Caumette P., Springer-Verlag, Heidelberg.

Chen G. H., Leong I. M., Liu J. and Huang J. C. (1999) Study of oxygen uptake by tidal river sediment. *Water Research* **33**(13), 2905-2912.

de Beer D., Schramm A., Santegoeds C. M. and Kühl M. (1997) A nitrite microsensor for profiling environmental biofilms. *Applied and Environmental Microbiology* **63**(3), 973-977.

Falkowski P. G. and Raven J. A. (1997a) Photosynthesis and primary production in nature. p. 263-299. In *Aquatic photosynthesis,* eds. Falkowski P. G. and Raven J. A., Blackwell Science, Malden, U.S.A.

Falkowski P. G. and Raven J. A. (1997b) Aquatic photosynthesis in biogeochemical cycles. p. 300-335. In *Aquatic photosynthesis,* eds. Falkowski P. G. and Raven J. A., Blackwell Science, Malden, U.S.A.

Feng H., Cochran J. K. and Hirschberg D. J. (2002) Transport and sources of metal contaminations over the course of tidal cycle in the turbidity maximum zone of the Hudson River estuary. *Water Research* **36**(3), 733-743.

Glud R. N., Ramsing N. B. and Revsbech N. P. (1992) Photosynthesis and photosynthesis-coupled respiration in natural biofilms quantified with oxygen microsensors. *Journal of phycology* **28**, 51-60.

Grötzschel S. and de Beer D. (2002) Effect of oxygen concentration on photosynthesis and respiration in two hypersaline microbial mats. *Microbial Ecology* **44**, 208-216.

Jensen K., Sloth N. P., Risgaard-Petersen N., Rysgaard S. and Revsbech N. P. (1994) Estimation of nitrification and denitrification from microprofiles of oxygen and nitrate in

model sediment systems. *Applied and Environmental Microbiology* **60**(6), 2094-2100.

Jørgensen B. B., Revsbech N. P., Blackburn T. H. and Cohen Y. (1979) Diurnal cycle of oxygen and sulfide microgradients and microbial photosynthesis in a cyanobacterial mat sediment. *Applied and Environmental Microbiology* **38**(1), 46-58.

Lorenzen J., Larsen L. H., Kjær T. and Revsbech N. P. (1998) Biosensor determination of the microscale distribution of nitrate, nitrate assimilation, nitrification, and denitrification in a diatom-inhabited freshwater sediment. *Applied and Environmental Microbiology* **64**(9), 3264-3269.

Murdroch A. and Azcue J. M. (1995) *Manual of aquatic sediment sampling*. Lewis publisher, U.S.A.

Okabe S., Itoh T., Satoh H. and Watanabe Y. (1999a) Analyses of spatial distributions of sulfate-reducing bacteria and their activity in aerobic wastewater biofilms. *Applied and Environmental Microbiology* **65**(11), 5107-5116.

Okabe S., Satoh H. and Watanabe Y. (1999b) In situ analysis of nitrifying biofilms as determined by in situ hybridization and the use of microelectrodes. *Applied and Environmental Microbiology* **65**(7), 3182-3191.

Ramsing N. B., Ferris M. J. and Ward D. M. (2000) Highly ordered vertical structure of *Synechococcus* populations within the one-millimeter-thick photic zone of a hot spring cyanobacterial mat. *Applied and Environmental Microbiology* **66**(3), 1038-1049.

Revsbech N. P. (1989) An oxygen microelectrode with a guard cathode. *Limnology and Oceanography* **34**, 474-478.

Revsbech N. P. and Jørgensen B. B. (1983) Photosynthesis of benthic microflora measured with high spatial resolution by the oxygen microprofile method: capabilities and limitations of the method. *Limnology and Oceanography* **28**(4), 749-756.

Revsbech N. P., Jørgensen B. B., Blackburn T. H. and Cohen Y. (1983) Microelectrode studies of the photosynthesis and O_2, H_2S, and pH profiles of a microbial mat. *Limnology and Oceanography* **28**(6), 1062-1074.

Revsbech N. P., Jørgensen B. B. and Brix O. (1981) Primary production of microalgae in sediments measured by oxygen microprofile, $H^{14}CO_3^-$ fixation, and oxygen exchanged methods. *Limnology and Oceanography* **26**(4), 717-730.

Satoh H., Nakamura Y., Ono H. and Okabe S. (2003) Effect of oxygen concentration on

nitrification and denitrification in single activated sludge flocs. *Biotechnology and Bioengineering* **83**(5), 604-607.

Sørensen J. and Revsbech N. P. (1990) Denitrification in stream biofilm and sediment: in situ variation and control factors. p. 277-289. In *Denitrification in soil and sediment. FEMS symposium no. 56,* eds. Revsbech N. P.and Sørensen J., Plenum Press, New York.

Ullman W. J. and Aller R. C. (1982) Diffusion coefficients in nearshore marine sediments. *Limnology and Oceanography* **27**(3), 552-556.

Wieland A. and Kühl M. (2000) Short-term temperature effects on oxygen and sulfide cycling in a hypersaline cyanobacterial mat (Solar Lake, Egypt). *Marine Ecology Progress Series* **196**, 87-102.

List of Figures

the gray area and dotted area, respectively.

Fig. 7. Mean steady-state O_2 concentration profiles (open circles) and calculated net rates of O_2 production and consumption (bars) in the sediment at the point 1. The O_2 concentrations were measured at light intensities of 10 (A), 400 (B), 1050 (C), 1550 (D), and 1900 (E) μmol photons/m^2/s. Error bars represent standard deviations of measurements. Positive and negative values indicate O_2 production and O_2 consumption rates, respectively. The microbial mat surface is at a depth of 0 μm. Microbial mat and sediment are indicated by the gray area and dotted area, respectively.

Fig. 8. Profiles of average gross photosynthetic rate (filled circles) and calculated O_2 respiration rate (open circles) in the sediment at the point 1 at 1900 μmol photons/m^2/s. Error bars represent standard deviations of measurements. Positive and negative values indicate O_2 production and O_2 respiration rates, respectively. The microbial mat surface is at a depth of 0 μm. Microbial mat and sediment are indicated by the gray area and dotted area, respectively.

Fig. 9. Representative steady-state O_2 concentration profiles (open circles) and calculated net rates of O_2 production and consumption (bars) in the sediment at the point 2. The O_2 concentrations were measured at light intensities of 10 (A), 100 (B), 400 (C), 730 (D), and 1250 (E) μmol photons/m^2/s. Positive and negative values indicate O_2 production and O_2 consumption rates, respectively. The microbial mat surface is at a depth of 0 μm. Microbial mat and sediment are indicated by the gray area and dotted area, respectively.

Fig. 10. The time course of O_2 concentration at a depth of 0.2 (A), 0.4 (B) and 0.6 (C) mm in the sediment at the point 1. The panel D shows a close-up view of the panel C in the elapsed time from 7130 to 7170 s. The sediment was artificially illuminated and shaded repeatedly. The shaded areas indicate periods of dark incubation. Note the expanded time scale in the panel A, B and D.

COD (mg/L)	BOD (mg/L)	DOC (mg/L)	NH_4^+ (µM)	NO_2^- (µM)	NO_3^- (µM)
16.8 ± 8.2	4.4 ± 2.0	11.2 ± 7.3	44 ± 39	1 ± 5	127 ± 168

O_2 (µM)	SO_4^{2-} (µM)	Salinity (%)	Temperature (˚C)	pH (-)
190 ± 40	3400 ± 3500	0.23 ± 0.24	17.4 ± 3.9	7.3 ± 0.8

Table 1
Photosynthesis in sediment determined at high spatial resolution by the use of microelectrodes
Yoshiyuki Nakamura et al.

Sample	Distance from the surface (mm)	Porosity (-)	Ds (10^{-5} cm^2/s)
Point 1	0-5	0.82 ± 0.09	1.40
	5-10	0.82 ± 0.07	1.41
	10-15	0.79 ± 0.06	1.31
	15-20	0.79 ± 0.08	1.30
	20-30	0.78 ± 0.07	1.27
	30-40	0.76 ± 0.09	1.20
	40-50	0.77 ± 0.11	1.23
	50-60	0.75 ± 0.11	1.18
Point 2	0-50	0.61 ± 0.04	0.78

Table 2
Photosynthesis in sediment determined at high spatial resolution by the use of microelectrodes
Yoshiyuki Nakamura et al.

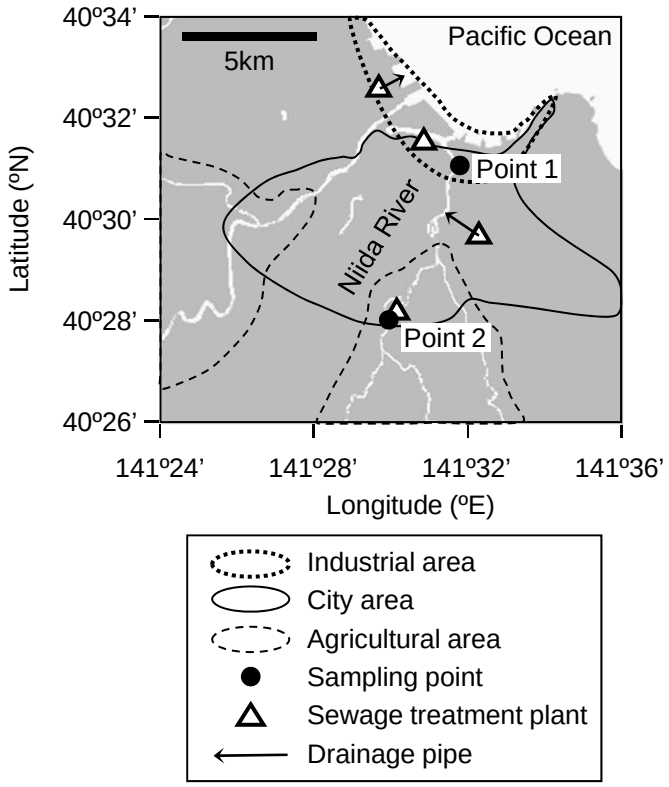

Fig. 1
Photosynthesis in sediments determined at high spatial resolution by the use of microelectrodes
Yoshiyuki Nakamura et al.

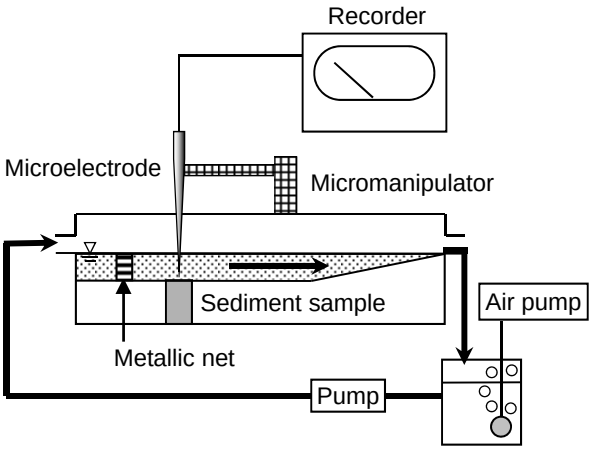

Fig. 2
Photosynthesis in sediments determined at high spatial resolution by the use of microelectrodes.
Yoshiyuki Nakamura et al.

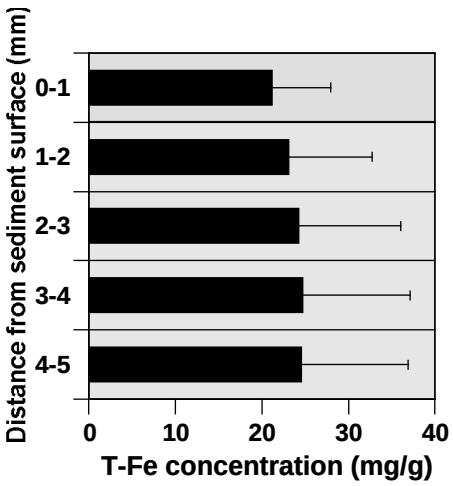

Fig. 3
Photosynthesis in sediment determined at high spatial resolution by the use of microelectrodes
Yoshiyuki Nakamura et al.

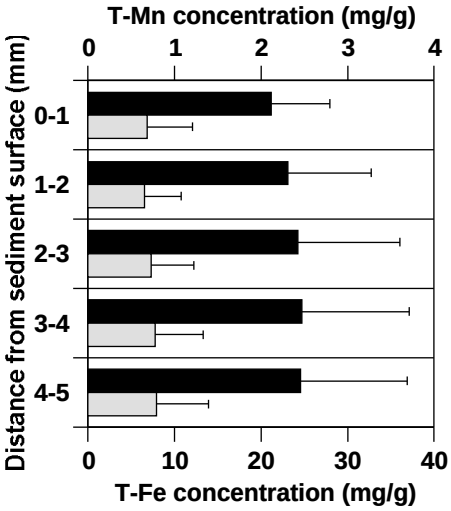

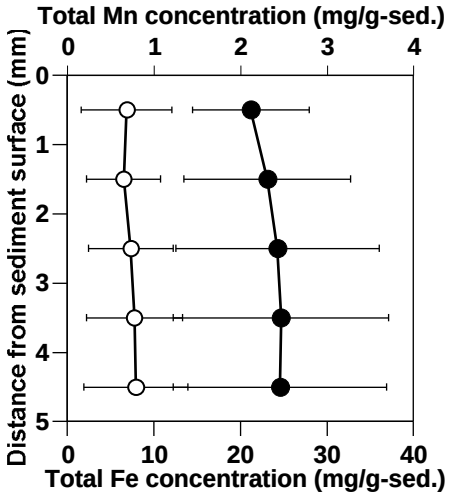

Fig.*

Macroscale.

Yoshiyuki Nakamura et al.

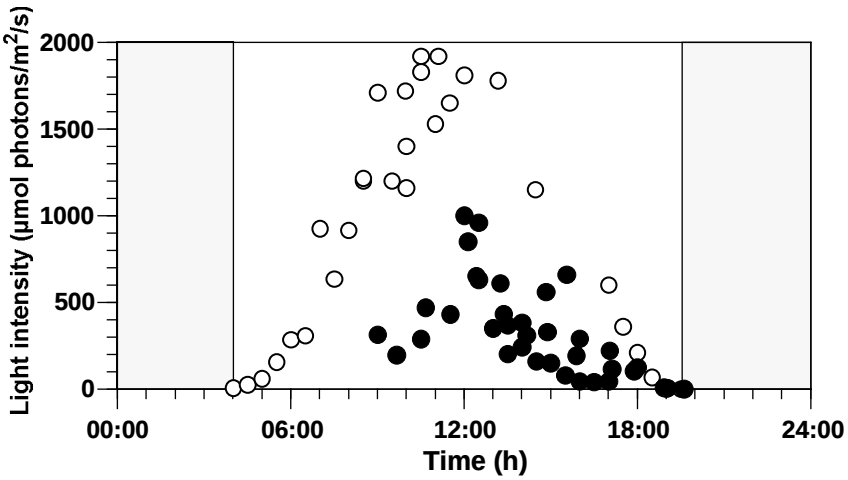

Fig. 4
Photosynthesis in sediment determined at high spatial resolution by the use of microelectrodes
Yoshiyuki Nakamura et al.

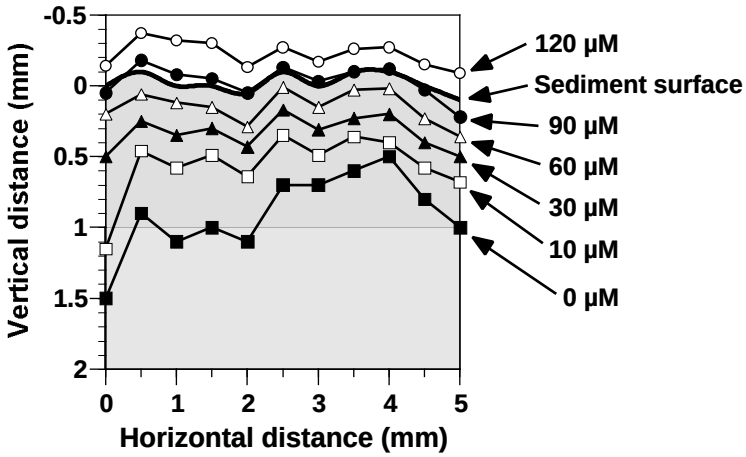

Fig. 5
Photosynthesis in sediment determined at high spatial resolution by the use of microelectrodes
Yoshiyuki Nakamura et al.

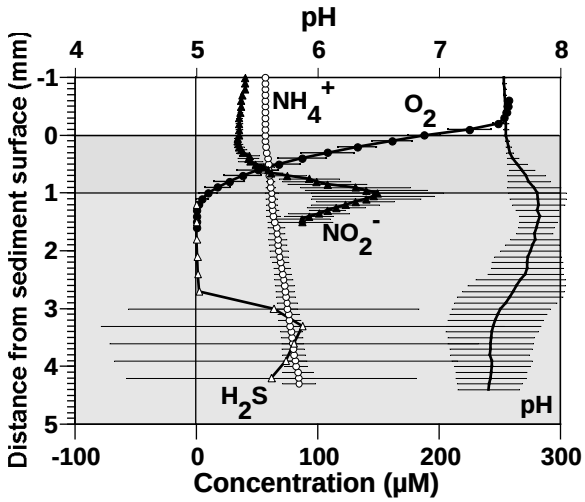

Fig. 6
Photosynthesis in sediment determined at high spatial resolution by the use of microelectrodes
Yoshiyuki Nakamura et al.

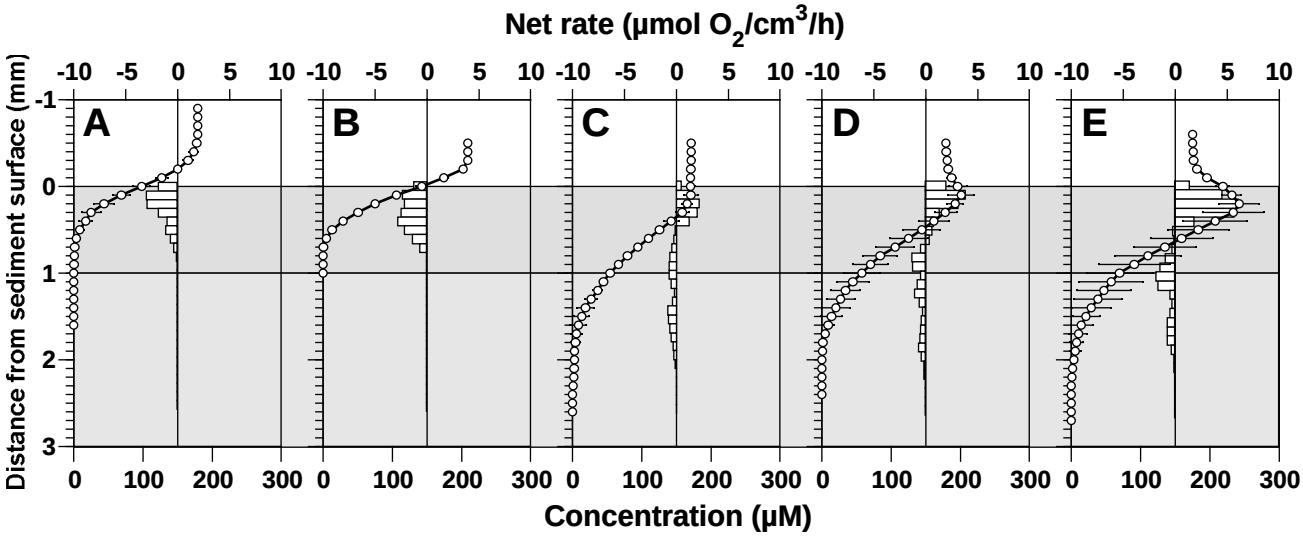

Fig. 7
Photosynthesis in sediment determined at high spatial resolution by the use of microelectrodes
Yoshiyuki Nakamura et al.

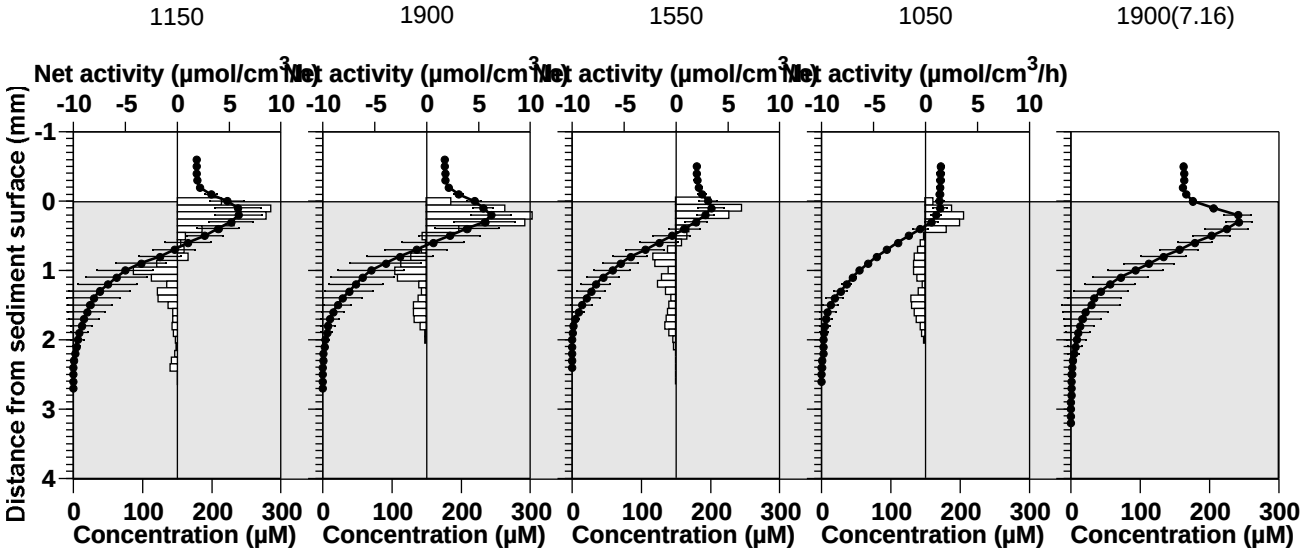

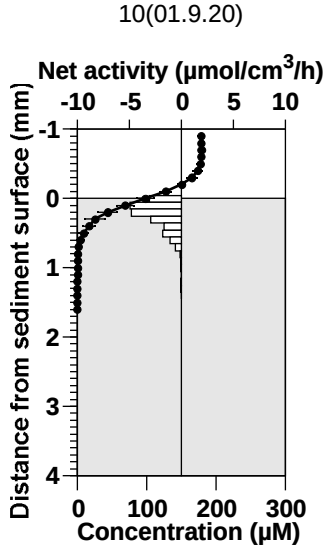

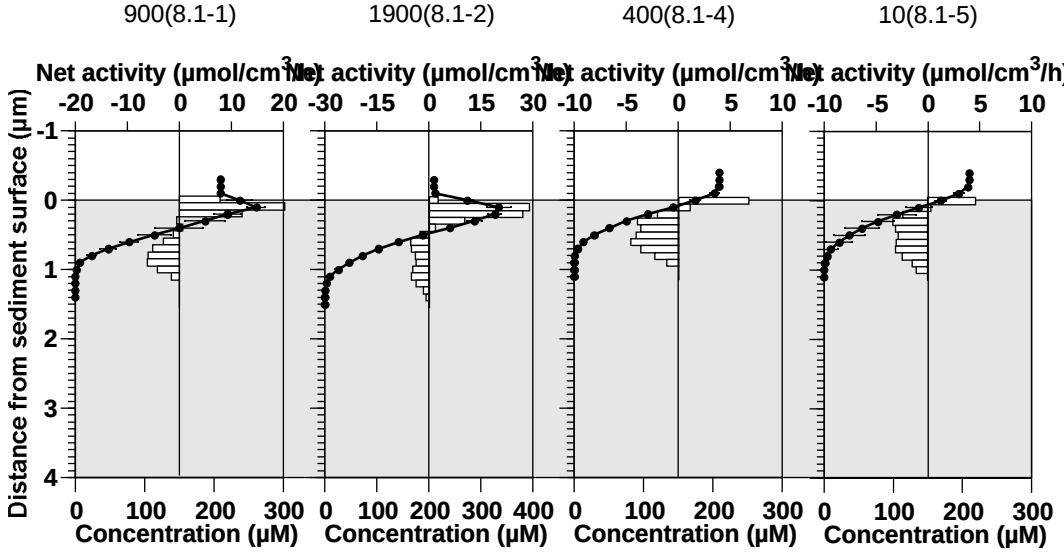

Fig.*

Macroscale.

Yoshiyuki Nakamura et al.

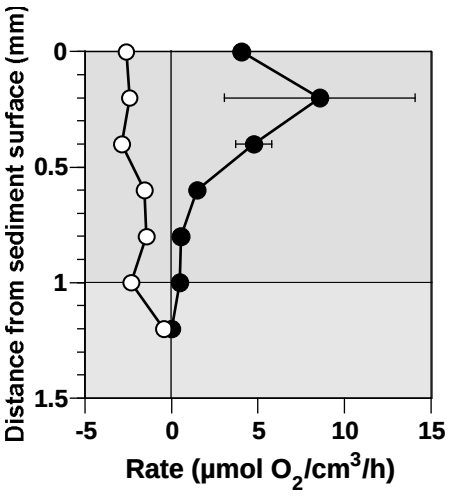

Fig. 8
Photosynthesis in sediment determined at high spatial resolution by the use of microelectrodes
Yoshiyuki Nakamura et al.

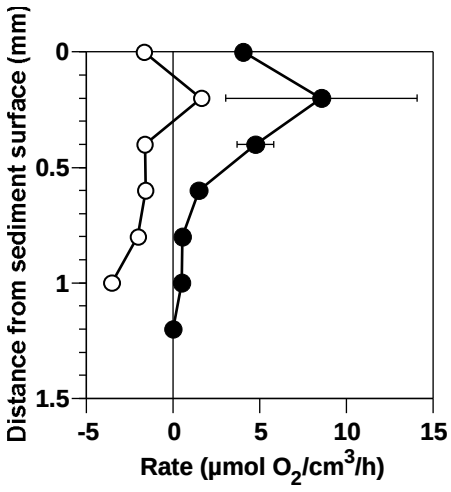

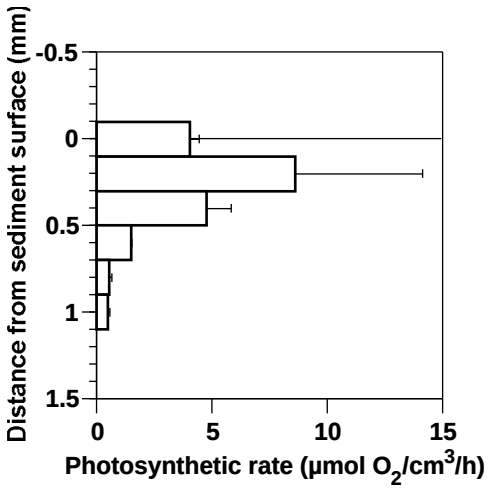

Fig.*

Macroscale.

Yoshiyuki Nakamura et al.

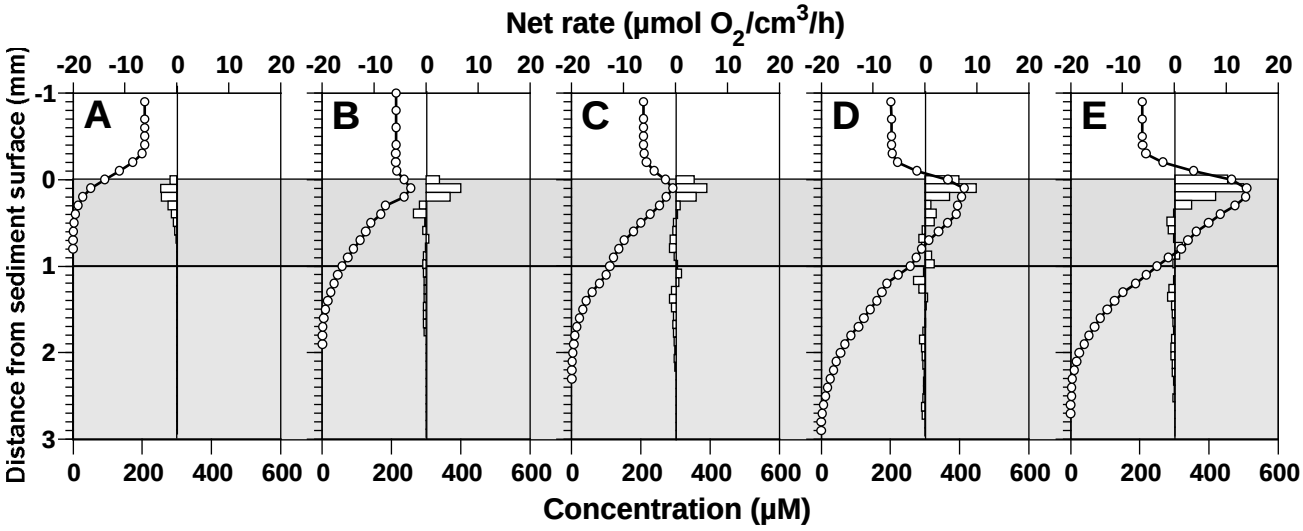

Fig. 9
Photosynthesis in sediment determined at high spatial resolution by the use of microelectrodes
Yoshiyuki Nakamura et al.

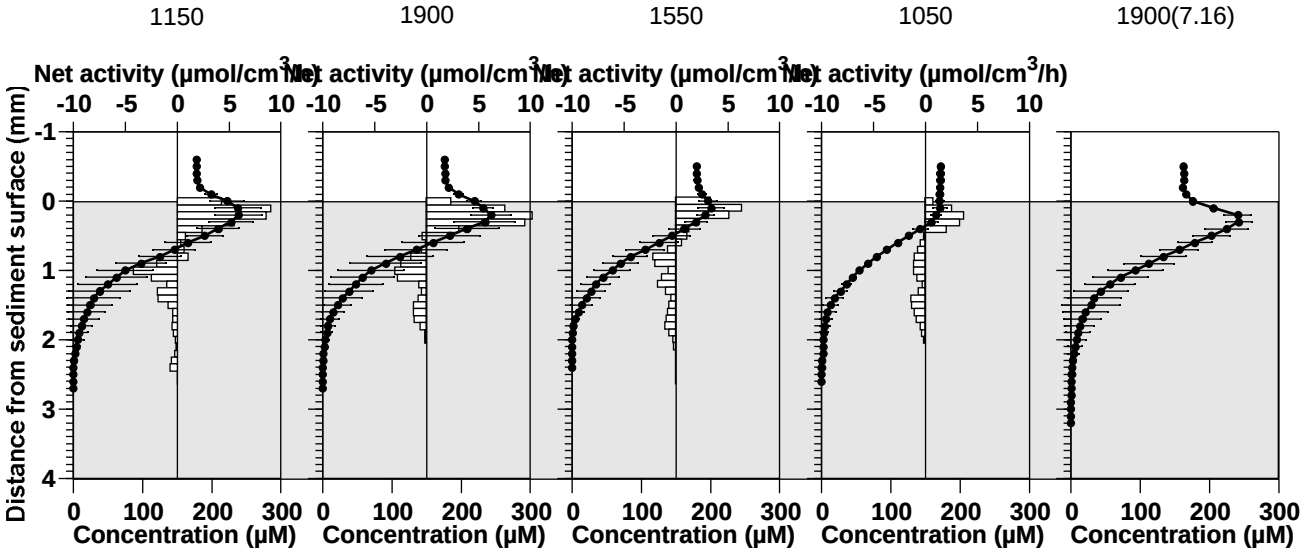

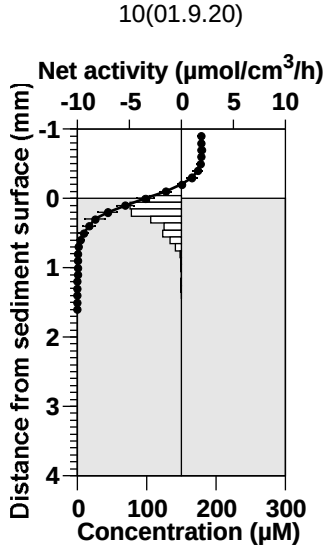

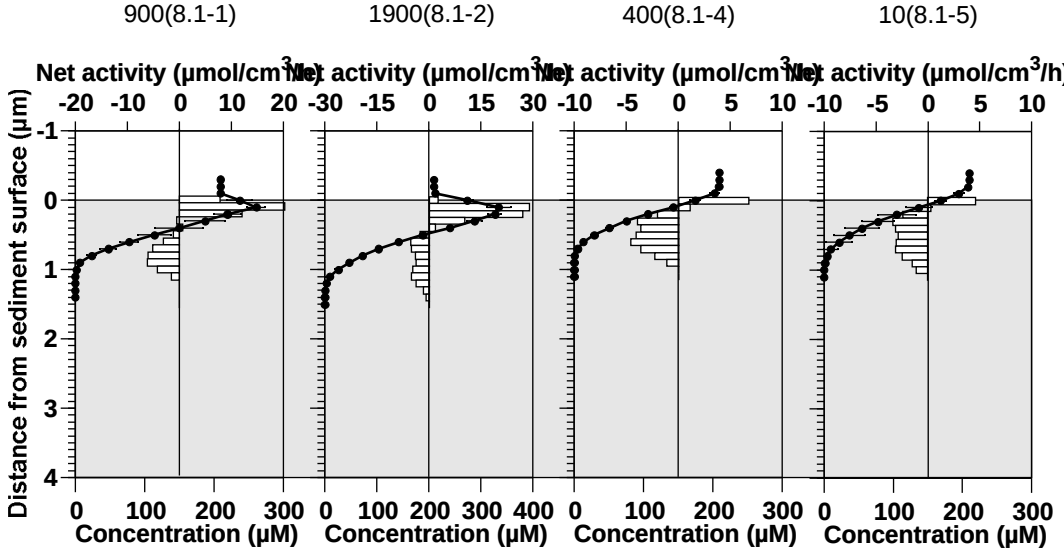

Fig.*

Macroscale.

Yoshiyuki Nakamura et al.

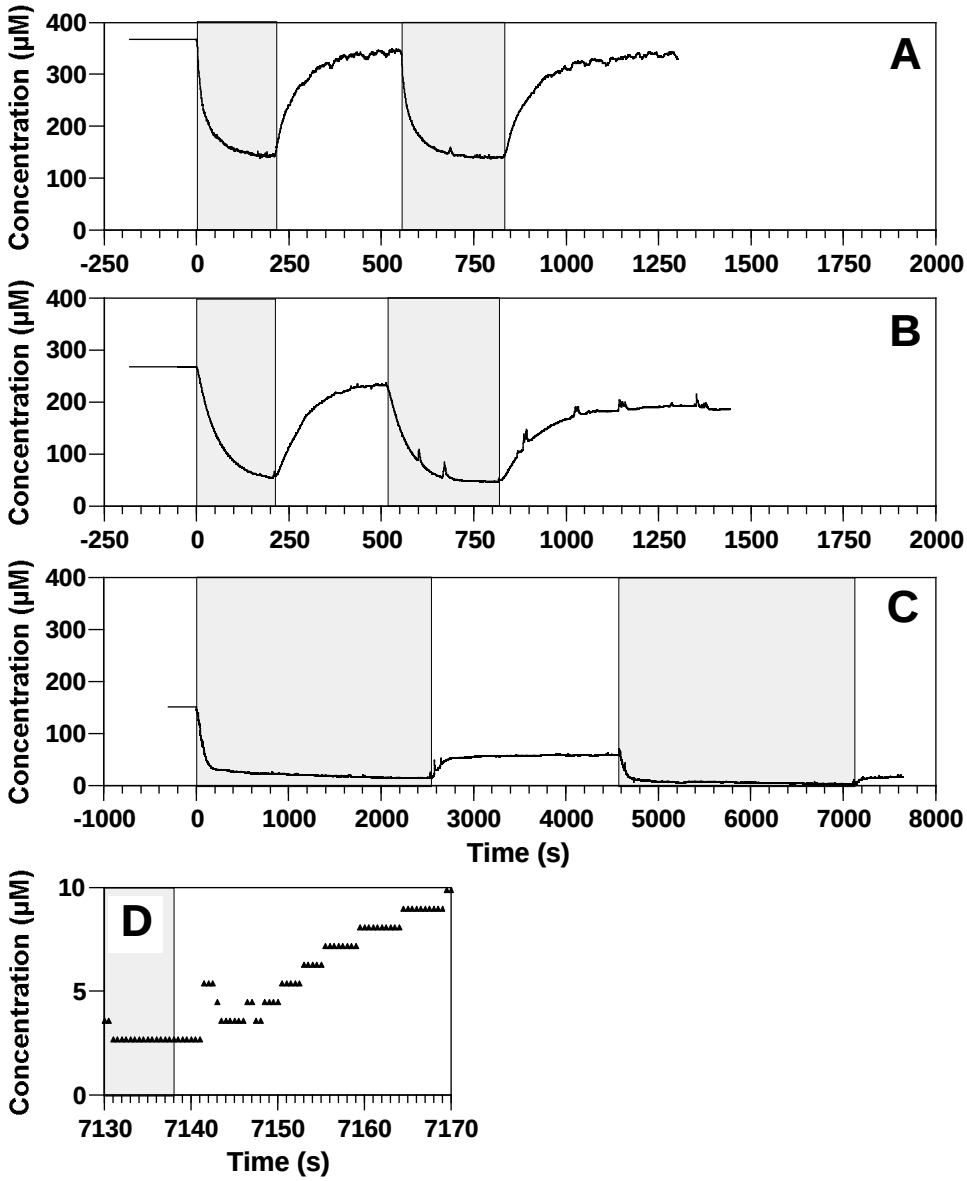

Fig. 10
Photosynthesis in sediment determined at high spatial resolution by the use of microelectrodes
Yoshiyuki Nakamura et al.